Modal parameters estimation in the Z-domain

Modal parameters estimation in the Z-domain

Alessandro Fasana

Politecnico di Torino, Dipartimento di Meccanica, Corso Duca degli Abruzzi, 24, I-10129 Torino Italy
Tel.: +39 011 0903397; fax: +39 011 0906999.
E-mail address: alessandro.fasana@polito.it

Keywords: Modal parameter; Z-domain; MIMO system; output only.

Abstract

This paper aims to explain in a clear, plain and detailed way a modal parameter estimation method in the frequency domain, or similarly in the Z-domain, valid for multi degrees of freedom systems. The technique is based on the Rational Fraction Polynomials (RFP) representation of the Frequency Response Function (FRF) of a Single Input Single Output (SISO) system but is simply extended to Multi Input Multi Output (MIMO) and output only problems. A least squares approach is adopted to take into account the information of all the FRFs but, when large data sets are used, the solution of the resulting system of algebraic linear equations can be a long and difficult task. A procedure to drastically reduce the problem dimensions is then adopted and fully explained; some practical hints are also given in order to achieve well conditioned matrices. The method is validated through numerical and experimental examples.

1. Introduction

In the past decades a number of papers dealing with the problem of modal parameters estimation of vibrating structures has been presented [1]. Even limiting the attention to linear systems, it is a matter of fact that both the complexity of the methods and the expectations of the analysts have increased and it is now compulsory to be able to cope with multi input multi output MIMO (and even output only) systems and large data sets. In the time domain, the Ibrahim time domain [2], the ARMAV [3] and the canonical variate analysis [4] methods have gained a certain popularity and proven their capabilities in a number of practical applications, see for example [5], but the

frequency domain techniques have always been more popular, mainly for the simplicity of a visual interpretation of the FRFs and the availability of effective commercial software. The common characteristic of many frequency domain methods is the description of the FRFs in terms of rational fraction polynomials(RFP) models [1], also known as common denominator models. Many efforts have been spent to pass from SIMO models [6] to MIMO (or even output only) models [7, 8] and indeed modifications and improvements are regularly proposed [9, 10]. Also this work takes start from the RFP representation and, with the aim of defining a small and well conditioned set of linear equations, describes a total least squares method in the Z-domain.

2. Outline of the RFP method in the *Z*-domain

For a linear and time invariant system with *n* degrees of freedom (dofs), the impulse response function can be expressed in the form [1]

$$h(t) = \sum_{r=1}^{2n} A_r e^{s_r t} \tag{1}$$

which gives the (continuous) Fourier transform

$$H(i\Omega) = \sum_{r=1}^{2n} \frac{A_r}{i\Omega - s_r} \tag{2}$$

The poles s_r, linked to the natural angular frequencies ω_r and damping ratios ζ_r by the expression $s_r = -\zeta_r\omega_r + i\omega_r\sqrt{1-\zeta_r^2}$, and the modal constants A_r are real or occur in pairs of complex conjugate numbers.

The Z transform of Eq. (1), whose left-hand side can numerically be computed by a discrete Fourier transform, taking into account a sampling frequency f_s and then a sampling period $\Delta t = 1/f_s$, is [1]

$$H_k = \sum_{r=1}^{2n} A_r \frac{z_k}{z_k - z_r} \tag{3}$$

where

$H_k = H(i\Omega_k)$, $\Omega_k = (k-1)\Delta\Omega = (k-1)2\pi\Delta f = \pi f_s (k-1)/(N-1)$,

Δf is the frequency resolution, *N* is the number of spectral lines and $k = 1,\ldots, N$.

The terms related to the Z transform are defined as

$$z_r = e^{s_r \Delta t}$$

$$z_k = e^{i(k-1)\Delta\Omega\,\Delta t} = e^{i\pi(k-1)/(N-1)} \tag{4}$$

It is worth to note that eq. (4) maps the frequency band under examination into a unit circle in the

Argand-Gauss plane.

The sum of eq. (3) can conveniently be converted in the following RFP expression

$$H_k = \frac{b_1 z_k + \ldots + b_{2n} z_k^{2n}}{a_0 + a_1 z_k + \ldots + a_{2n-1} z_k^{2n-1} + z_k^{2n}} \tag{5}$$

where the $4n$ unknown coefficients $a_0,\ldots,a_{2n-1}$ and $b_1,\ldots,b_{2n}$ are real valued [1].

Expanding eq. (5) for N spectral lines it is simple to get

$$\begin{bmatrix} H_1 & H_1 z_1 & \ldots & H_1 z_1^{2n-1} \\ H_2 & H_2 z_2 & \ldots & H_2 z_2^{2n-1} \\ \vdots & \vdots & \ddots & \vdots \\ H_N & H_N z_N & \ldots & H_N z_N^{2n-1} \end{bmatrix} \begin{Bmatrix} a_0 \\ a_1 \\ \vdots \\ a_{2n-1} \end{Bmatrix} - \begin{bmatrix} z_1 & z_1^2 & \ldots & z_1^{2n} \\ z_2 & z_2^2 & \ldots & z_2^{2n} \\ \vdots & \vdots & \ddots & \vdots \\ z_N & z_N^2 & \ldots & z_N^{2n} \end{bmatrix} \begin{Bmatrix} b_1 \\ b_2 \\ \vdots \\ b_{2n} \end{Bmatrix} = - \begin{Bmatrix} H_1 z_1^{2n} \\ H_2 z_2^{2n} \\ \vdots \\ H_N z_N^{2n} \end{Bmatrix} \tag{6}$$

or, in a more compact form

$$\mathbf{Aa} - \mathbf{Bb} = \mathbf{w} \tag{7}$$

$$\begin{bmatrix} \mathbf{A} & -\mathbf{B} \end{bmatrix} \begin{Bmatrix} \mathbf{a} \\ \mathbf{b} \end{Bmatrix} = \mathbf{w}$$

By taking $N \geq 4n$ the previous system of linear equations can be solved in a least square sense, for example by a singular value decomposition, to give **a** and **b**.

It would also possible to properly weight with W_k each FRF value H_k [10] in order to increase the importance of some spectral lines, typically in proximity of the system resonances. This would lead to different **A** and **w** but leave **B** unchanged, which is important for the forthcoming discussion.

When another FRF is considered, matrix **B** and vector **a** of eq. (7) remain unchanged so that, with NFRF frequency response functions, a system of equations can be assembled in the form

$$\begin{bmatrix} \mathbf{A}_1 \\ \vdots \\ \mathbf{A}_{NFRF} \end{bmatrix} \mathbf{a} + \begin{bmatrix} -\mathbf{B} & \ldots & \mathbf{0} \\ \vdots & \ddots & \vdots \\ \mathbf{0} & \ldots & -\mathbf{B} \end{bmatrix} \begin{Bmatrix} \mathbf{b}_1 \\ \vdots \\ \mathbf{b}_{NFRF} \end{Bmatrix} = \begin{Bmatrix} \mathbf{w}_1 \\ \vdots \\ \mathbf{w}_{NFRF} \end{Bmatrix} \tag{8}$$

It may be observed that this equation holds true also for MIMO systems, being the coefficients **a** (related to the poles s_r) independent from both the excitation and measurement points.

The system of eq. (8) has $2n(NFRF+1)$ unknowns, i.e. the elements of the vectors **a** and $\mathbf{b}_m$, m=1,…,NFRF, and again can be solved in a least square sense by taking in each FRF enough spectral lines N: in particular $N \geq 2n(1+1/NFRF)$. The above procedure is indeed correct but can lead to a very time consuming implementation, especially when large data sets are analysed (NFRF>>1) and n has to vary (e.g. to define a stabilization chart).

It is then necessary and interesting to develop an alternative process, still based on a least square procedure but numerically much more efficient.

For the mth generic FRF, eq. (7) can also be written in the form

$$\mathbf{A}_m\mathbf{a} - \mathbf{B}\mathbf{b}_m - \mathbf{w}_m = \mathbf{e}_m$$

where vector $\mathbf{e}_m$ takes into account the errors between the measured FRF and the assumed model. In order to compute the unknown vectors **a** and $\mathbf{b}_m$ the least squares procedure requires to minimise the real valued (positive) function $E_m = \mathbf{e}_m^H\mathbf{e}_m$: therefore E_m is the sum of the errors occurring on all the N spectral lines of the m[th] FRF. With NFRF frequency response functions, one for each combination of the input and output measurement points, it is then natural to define the global error *E* as

$$E = \sum_{m=1}^{NFRF} E_m .$$

According this definition *E* is real valued, and so are **a** and the $\mathbf{b}_m$, so that its explicit expression is

$$E = \sum_{m=1}^{NFRF} \mathbf{e}_m^H\mathbf{e} = \mathrm{Re}\sum_{m=1}^{NFRF}\left[\left(\mathbf{A}_m\mathbf{a} - \mathbf{B}\mathbf{b}_m - \mathbf{w}_m\right)^H\left(\mathbf{A}_m\mathbf{a} - \mathbf{B}\mathbf{b}_m - \mathbf{w}_m\right)\right]$$

and also

$$\begin{aligned} E = &\sum_{m=1}^{NFRF}\left(\mathbf{a}^T\,\mathrm{Re}\left[\mathbf{A}_m^H\mathbf{A}_m\right]\mathbf{a} - \mathbf{a}^T\,\mathrm{Re}\left[\mathbf{A}_m^H\mathbf{B}\right]\mathbf{b}_m - \mathbf{a}^T\,\mathrm{Re}\left[\mathbf{A}_m^H\mathbf{w}_m\right]\right) + \\ &+ \sum_{m=1}^{NFRF}\left(-\mathbf{b}_m^T\,\mathrm{Re}\left[\mathbf{B}^H\mathbf{A}_m\right]\mathbf{a} + \mathbf{b}_m^T\,\mathrm{Re}\left[\mathbf{B}^H\mathbf{B}\right]\mathbf{b}_m + \mathbf{b}_m^T\,\mathrm{Re}\left[\mathbf{B}^H\mathbf{w}_m\right]\right) + \\ &+ \sum_{m=1}^{NFRF}\left(-\mathrm{Re}\left[\mathbf{w}_m^T\mathbf{A}_m\right]\mathbf{a} + \mathrm{Re}\left[\mathbf{w}_m^T\mathbf{B}\right]\mathbf{b}_m + \mathbf{w}_m^T\mathbf{w}_m\right) \end{aligned}$$

E is minimum, as a function of **a** and the $\mathbf{b}_m$, when $\partial E/\partial\mathbf{a} = 0$ and $\partial E/\partial\mathbf{b}_m = 0$, m = 1,…, *NFRF*.

Remember now that, for any generic **x**, **z** and **Y**, the derivation rules state that

$$\begin{aligned} \partial\left(\mathbf{x}^T\mathbf{Y}\,\mathbf{z}\right)/\partial\mathbf{x} &= \mathbf{Y}\,\mathbf{z} \\ \partial\left(\mathbf{x}^T\mathbf{Y}\,\mathbf{z}\right)/\partial\mathbf{z} &= \mathbf{Y}\,\mathbf{x} \end{aligned} \qquad (9)$$

so that the condition for minimising *E* is expressed by

$$\frac{\partial E}{\partial\mathbf{a}} = 2\sum_{m=1}^{NFRF}\left(\mathrm{Re}\left[\mathbf{A}_m^H\mathbf{A}_m\right]\mathbf{a} - \mathrm{Re}\left[\mathbf{A}_m^H\mathbf{B}\right]\mathbf{b}_m - \mathrm{Re}\left[\mathbf{A}_m^H\mathbf{w}_m\right]\right) = 0 \qquad (10)$$

$$\frac{\partial E}{\partial\mathbf{b}_m} = -2\,\mathrm{Re}\left[\mathbf{B}^H\mathbf{A}_m\right]\mathbf{a} + 2\,\mathrm{Re}\left[\mathbf{B}^H\mathbf{B}\right]\mathbf{b}_m + 2\,\mathrm{Re}\left[\mathbf{B}^H\mathbf{w}_m\right] = 0 \qquad (11)$$

In eq. (11) the sum is not present because each vector $\mathbf{b}_m$ is independent from all the others $\mathbf{b}_p$ ($p = 1,\ldots,NFRF, p \neq m$) so that one can obtain

$$\mathbf{b}_m = \left(\mathrm{Re}\left[\mathbf{B}^H\mathbf{B}\right]\right)^{-1}\left(\mathrm{Re}\left[\mathbf{B}^H\mathbf{A}_m\right]\mathbf{a} - \mathrm{Re}\left[\mathbf{B}^H\mathbf{w}_m\right]\right) \qquad (12)$$

where $\mathrm{Re}\left[\mathbf{B}^H\mathbf{B}\right] \in \Re^{2n\times 2n}$.

A back substitution in eq. (10) gives

$$\sum_{m=1}^{NFRF}\left(\mathrm{Re}\left[\mathbf{A}_m^H\mathbf{A}_m\right]-\mathrm{Re}\left[\mathbf{A}_m^H\mathbf{B}\right]\left(\mathrm{Re}\left[\mathbf{B}^H\mathbf{B}\right]\right)^{-1}\mathrm{Re}\left[\mathbf{B}^H\mathbf{A}_m\right]\right)\mathbf{a} = \\ = \sum_{m=1}^{NFRF}\left(\mathrm{Re}\left[\mathbf{A}_m^H\mathbf{w}_m\right]-\mathrm{Re}\left[\mathbf{A}_m^H\mathbf{B}\right]\left(\mathrm{Re}\left[\mathbf{B}^H\mathbf{B}\right]\right)^{-1}\mathrm{Re}\left[\mathbf{B}^H\mathbf{w}_m\right]\right) \qquad (13)$$

or in brief

$$\mathbf{R}\,\mathbf{a} = \mathbf{r} \qquad (14)$$

with $\mathbf{R}\in\Re^{2n\times 2n}$ and $\mathbf{r}\in\Re^{2n\times 1}$.

A very important result is thus achieved: a system of only 2n real linear equations has to be solved for **a**, but based on all the N spectral lines of NFRF frequency response functions. Both **R** and **r** are defined as simple sums whose terms only contain the product of matrices, which is a numerically simple task. Moreover, because of the formulation in the Z domain, matrix **R** is well conditioned and eq. (14) achieve a reliable evaluation of vector **a**.

Some difficulties could arise in the computation of $\left(\mathrm{Re}\left[\mathbf{B}^H\mathbf{B}\right]\right)^{-1}$ but a closer look to the structure of the matrix shows that this inversion is straightforward. Taking into account –eq. (4)- that $\left(z_k^j\right)^* = z_k^{-j}$, the generic element at line *j* and column *l* of matrix $\mathbf{B}^H\mathbf{B}$, namely B^HB_{jl}, is given by

$$B^HB_{jl} = \left\{z_1^{-j} \quad z_2^{-j} \quad \dots \quad z_N^{-j}\right\}\left\{z_1^{l} \quad z_2^{l} \quad \dots \quad z_N^{l}\right\}^T = \sum_{k=1}^{N} z_k^{l-j} = \sum_{k=1}^{N} e^{i\pi(l-j)(k-1)/(N-1)}$$

The last sum gives

$$\mathrm{Re}\left(B^HB_{jl}\right) = \sum_{k=1}^{N}\cos\left(\pi(l-j)(k-1)/(N-1)\right) =$$

$$= \cos(0) + \cos(\pi(l-j)/(N-1)) + \ldots + \cos\left(\pi(l-j)(N-2)/(N-1)\right) + \cos\left(\pi(l-j)\right)$$

By remembering the symmetry properties of the harmonic function, the conclusion is

$\mathrm{Re}\left(B^HB_{jl}\right) = N$ if $l = j$;

$\mathrm{Re}\left(B^HB_{jl}\right) = 1$ if $|l-j|$ is even

$\mathrm{Re}\left(B^HB_{jl}\right) = 0$ if $|l-j|$ is odd

On this basis we get

$$\mathrm{Re}\left[\mathbf{B}^H\mathbf{B}\right]=\begin{bmatrix} N & 0 & 1 & 0 & \dots & 1 & 0 \\ 0 & N & 0 & 1 & \dots & 0 & 1 \\ 1 & 0 & N & 0 & \dots & 1 & 0 \\ 0 & 1 & 0 & N & \dots & 0 & 1 \\ \vdots & \vdots & \vdots & \vdots & \ddots & \vdots & \vdots \\ 1 & 0 & 1 & 0 & \dots & N & 0 \\ 0 & 1 & 0 & 1 & \dots & 0 & N \end{bmatrix}$$

which allows to calculate

$$\left(\mathrm{Re}\left[\mathbf{B}^H\mathbf{B}\right]\right)^{-1}=\frac{1}{den}\begin{bmatrix} num & 0 & -1 & 0 & \dots & -1 & 0 \\ 0 & num & 0 & -1 & \dots & 0 & -1 \\ -1 & 0 & num & 0 & \dots & -1 & 0 \\ 0 & -1 & 0 & num & \dots & 0 & -1 \\ \vdots & \vdots & \vdots & \vdots & \ddots & \vdots & \vdots \\ -1 & 0 & -1 & 0 & \dots & num & 0 \\ 0 & -1 & 0 & -1 & \dots & 0 & num \end{bmatrix} \qquad (15)$$

with $num = N + n - 2$ and $den = N^2 + (n-2)N - n + 1$

Therefore the definition of all the terms of eq. (13), which is the core of the procedure, does not present any numerical difficulty and provides a well conditioned matrix **R** in eq. (14).

Eq. (14) gives **a** so that the poles $s_r = \ln z_r / \Delta t$ of the system can be obtained by computing the solutions z_r, r=1,…,2n, of the following equation:

$$a_0 + a_1 z + \dots + a_{2n-1} z^{2n-1} + z^{2n} = 0 \qquad (16)$$

i.e. by determining the zeros z_r of a polynomial.

Given **a**, any vector $\mathbf{b}_m$, and consequently the related modal constants A_r, could be obtained with the products of eq. (12). But for the modal constants, as well as for the poles, it is more convenient to implemented a least square procedure, again on the basis of eq. (3). By considering a single FRF, for any k (frequency) and r (pole), it is now simple to compute the ratio $N_{kr} = z_k / (z_k - z_r)$ and a system of equations can be written as

$$\begin{Bmatrix} H_1 \\ \vdots \\ H_N \end{Bmatrix} = \begin{bmatrix} N_{11} & \dots & N_{1\,2n} \\ \vdots & \ddots & \vdots \\ N_{N1} & \dots & N_{N\,2n} \end{bmatrix} \begin{Bmatrix} A_1 \\ \vdots \\ A_{2n} \end{Bmatrix} \qquad (17)$$

or, in brief

$$\mathbf{H} = \mathbf{N}\mathbf{A} \qquad (18)$$

With $N \geq 2n$ the previous system of complex linear equations could be solved in a least square sense to give complex coefficients **A** (A_r, r=1,…,2n) but it is again possible to limit the number of

simultaneous equations by separately searching for the real and imaginary parts of **A**, respectively $\mathbf{R}_A$ and $\mathbf{I}_A$. Eq. (18) is then written in the form

$$\mathbf{N}\,\mathbf{R}_A + i\,\mathbf{N}\,\mathbf{I}_A - \mathbf{H} = \boldsymbol{\varepsilon}$$

where $\boldsymbol{\varepsilon}$ is the error vector.

According to eq (9), by minimising the error $e = \boldsymbol{\varepsilon}^{\mathbf{H}}\boldsymbol{\varepsilon}$ with respect to $\mathbf{R}_A$ and $\mathbf{I}_A$, the following system of linear equations is found

$$\begin{bmatrix} \mathrm{Re}\left[\mathbf{N}^H\mathbf{N}\right] & \mathrm{Re}\left[i\,\mathbf{N}^H\mathbf{N}\right] \\ \mathrm{Re}\left[i\,\mathbf{N}^H\mathbf{N}\right] & -\mathrm{Re}\left[\mathbf{N}^H\mathbf{N}\right] \end{bmatrix} \begin{Bmatrix} \mathbf{R}_A \\ \mathbf{I}_A \end{Bmatrix} = \begin{Bmatrix} \mathrm{Re}\left[\mathbf{N}^H\mathbf{H}\right] \\ \mathrm{Re}\left[i\,\mathbf{N}^H\mathbf{H}\right] \end{Bmatrix} \tag{19}$$

or, briefly

$$\begin{bmatrix} \mathbf{G_1} & \mathbf{G_2} \\ \mathbf{G_2} & -\mathbf{G_1} \end{bmatrix} \begin{Bmatrix} \mathbf{R}_A \\ \mathbf{I}_A \end{Bmatrix} = \begin{Bmatrix} \mathbf{b_1} \\ \mathbf{b_2} \end{Bmatrix}$$

The second equation gives

$$\mathbf{R}_c = \mathbf{G_2}^{-1}\left(\mathbf{G_1}\,\mathbf{I}_c + \mathbf{b_2}\right) \tag{20}$$

and then, from the first equation

$$\left(\mathbf{G_1}\,\mathbf{G_2}^{-1}\,\mathbf{G_1} + \mathbf{G_2}\right)\mathbf{I}_A = \mathbf{b_1} - \mathbf{G_1}\,\mathbf{G_2}^{-1}\,\mathbf{b_2} \tag{21}$$

This simple system of *2n* real equations yields $\mathbf{I}_A$ so that by with a direct substitution in eq. (20) also $\mathbf{R}_A$ is determined.

In a nutshell the whole process, which will be named RFPZ method, just requires these few steps:

- build up matrices $\mathbf{A}_m$ and $\mathbf{B}$ and vectors $\mathbf{w}_m$ according to eqs. (6) and (8);
- compute vector **a** with eq. (14) , with the help of eqs. (13) and (15);
- compute the zeros z_r of eq. (16) and then the poles s_r with eq. (4);
- compute the imaginary and real parts of the modal constants **A**, and then the mode shapes, with eqs. (21) and (20).

3.Numerical examples

To demonstrate the effectiveness of the RFPZ technique, a seven degrees of freedom system with non proportional viscous damping has been numerically simulated. Table 1 reports its natural frequencies and damping ratios; the eigenvectors are not listed for brevity and because they will be compared with the extracted mode shapes only by means of the Modal Assurance Criterion (MAC). The input was a white noise applied on mass 2 and the outputs were computed in the form of displacements of the seven dofs, for a duration of 200 s and with a sampling frequency of 256 Hz . The fourth order Runge-Kutta integration technique implemented in Matlab® (ODE4) has been

chosen for all the computations.

The FRFs have been computed with the Welsh's periodogram method, 4096 spectral lines (giving a frequency resolution Δf=0.0625 Hz), a sine window and an overlap of 66% [11]. Figure 1 shows an example of seven frequency response functions.

With regard to the extracted modal parameters, the results herewith presented have been obtained on the basis of a Montecarlo simulation consisting of 100 repetitions of the whole process of input generation, time domain integration, FRFs computation and modal parameters evaluation.

Some words need to be spent on the rationale that allows to separate physical and numerical modes. First of all it is worth remembering that the number of modes of a system is in general not know a priori so that it is necessary to presume which model order *n* allows the best fitting of the measured data. The typical procedure starts from a low *n* (possibly *n*=1) and increases its value up to an arbitrary limit that depends on various factors among which the user's experience is not to be neglected. The result of this practice is a number of modes, with the physical (true) to be split from the computational ones. One possible, and certainly practical and diffused, approach consists in the generation and observation of the so called stabilisation chart or diagram [7].

Table 1

Natural frequencies and damping ratios of the numerical example

Mode number k	1	2	3	4	5	6	7
f_k (Hz)	3.398	10.45	18.54	22.59	24.66	28.63	38.48
ζ_k (%)	0.361	0.875	1.49	1.88	1.82	1.68	2.35

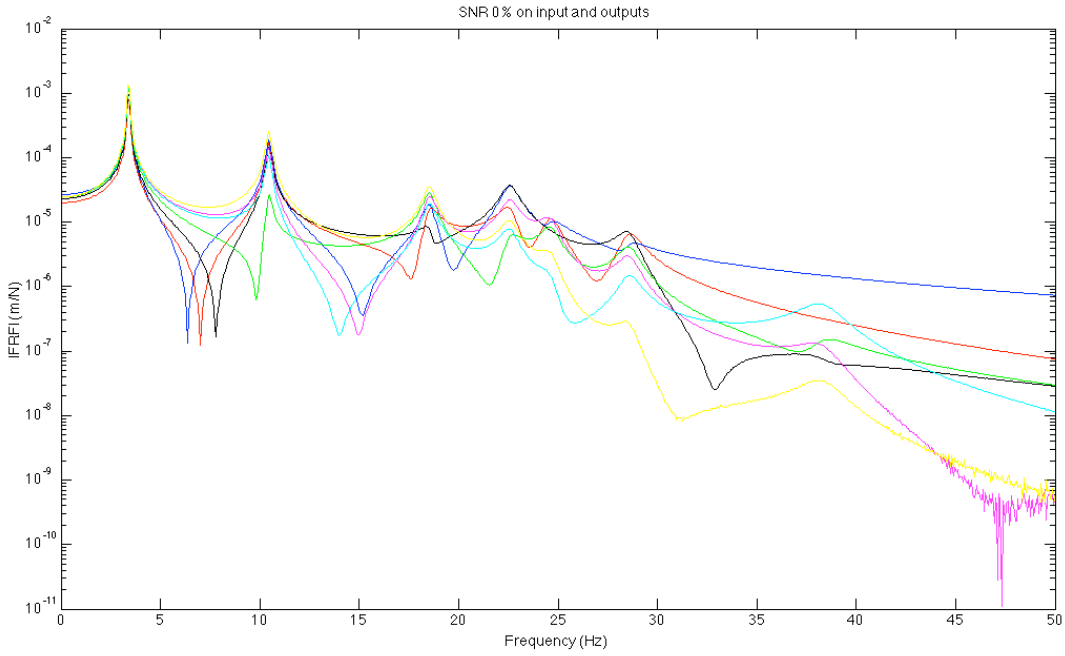

Fig. 1. Example of FRFs (receptance) with no added noise, e ¼ 0.

To accomplish this task the method implemented in this paper is slightly different. The stabilisation chart is in fact substituted by an histogram (Fig. 2); the number of repetitions of a pole, computed with different model orders *n*, is plotted as a function of frequency (it is of great help to exclude from this graph the non physical poles, estimated with negative damping ratios). Stable, and hopefully physical, modes give well defined and high bars in the histogram (Fig. 2, left). In presence of a high valued bar, the choice of the mode (frequency, damping ratio, shape) is then performed by evaluating the MAC among all the mode shapes, one for each pole within the frequency limits of the bar. The mode shape which, in the MAC sense, is most similar to all the others is considered the most representative and its pole is then the "best" pole. This approach can be more cumbersome than simply picking a stable mode in a stabilisation chart but is convenient to keep the whole procedure less sensitive to personal opinions. And, in general, the time dedicated to the preparation and execution of the experimental tests, and their subsequent interpretation, is much larger than the computational effort required by any fitting procedure.

The tables of results in this paper list the modal parameters (and their standard deviations) produced by processing, according to the above procedure, the already mentioned 100 simulations.

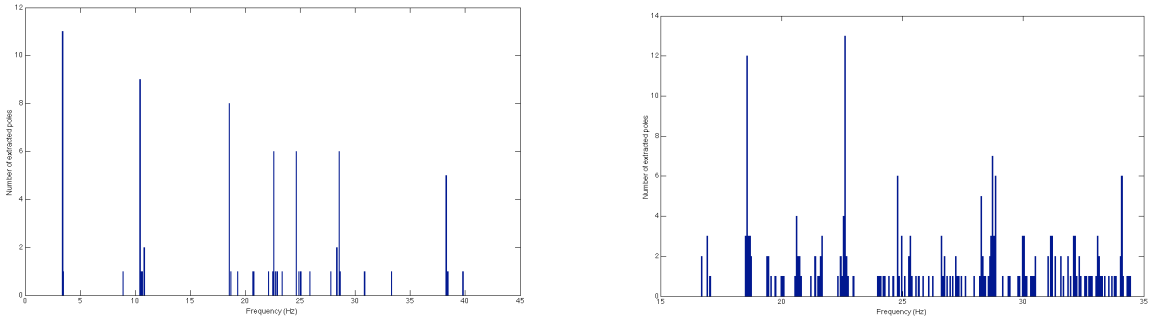

Fig. 2. Examples of the histogram plot. Left: SIMO system with no added noise. Right: SIMO system with 10% added noise.

Table 2

Modal parameters and their standard deviations: no added noise (receptance)

Mode number k	1	2	3	4	5	6	7
f_k (Hz)	3.399	10.45	18.54	22.57	24.64	28.58	38.31
σ_f (Hz)	0.002	0.01	0.00	0.01	0.04	0.00	0.06
ζ_k (%)	1.073	1.037	1.605	2.021	2.009	1.854	2.893
σ_ζ (%)	0.056	0.10	0.01	0.02	0.30	0.00	0.08
MAC	1.000	1.000	0.999	0.998	0.990	0.981	0.067
σ_{MAC}	0.000	0.000	0.001	0.002	0.013	0.033	0.090

Frequency band: 1–45 Hz; maximum model order: 15.

The presence of noise corrupting the signals has been simulated by adding, after the numerical integration, on both the input and the outputs different sequences of white noise, with Gaussian distribution, null mean value and unitary standard deviation. In practice the noisy signal $x(t)_{noisy}$ is given by $x(t)_{noisy} = x(t) + e\,\sigma_x\,n(t)$ where $x(t)$ and σ_x are the original signal and its standard deviation, $n(t)$ is the white noise and e is a parameter controlling the signal to noise ratio.

The values in Table 2 have been obtained without adding any noise on the input and the outputs, and by analysing the FRFs in the frequency band 1-45 Hz with a maximum model order *n*=15. The results for the first six modes are quite satisfactory, with some significant errors occurring only on the damping ratios of modes one and two. These errors are caused by the combination of the small values of damping ratios, which generate sharp peaks in the FRFs, and the frequency resolution, which is not small enough to correctly define these peaks. The large error on mode shape seven can be justified by observing in Figure 1 the FRFs in the frequency band corresponding to this mode (35-40 Hz); they are a couple of orders of magnitude lower than in the remaining frequency region and mode seven is then masked by the other modes. In fact, by repeating the identification procedure on inertances instead of receptances, the MAC on mode seven increases to 0.996 with standard deviation 0.006.

When noise (10% on both the input and the outputs) is added on the time histories also the resulting FRFs get noisy, as shown for example in Figure 3. Table 3 lists the modal parameters extracted by processing these receptances in the band 15-35 Hz with a maximum model order *n*=25. The MAC is calculated between the extracted and the theoretical mode shapes.

The frequency band is smaller than before to consider the realistic situation of unmeasured but present modes (one and two in this case) and also because mode seven has already been judged too small to be properly detected. The noise effects are clearly visible on the histogram of Figure 2 (right) where it is no more simple to separate physical and computational modes. It is also evident that the damping ratio is largely influenced by the noise even if both frequency and mode shape are correctly defined.

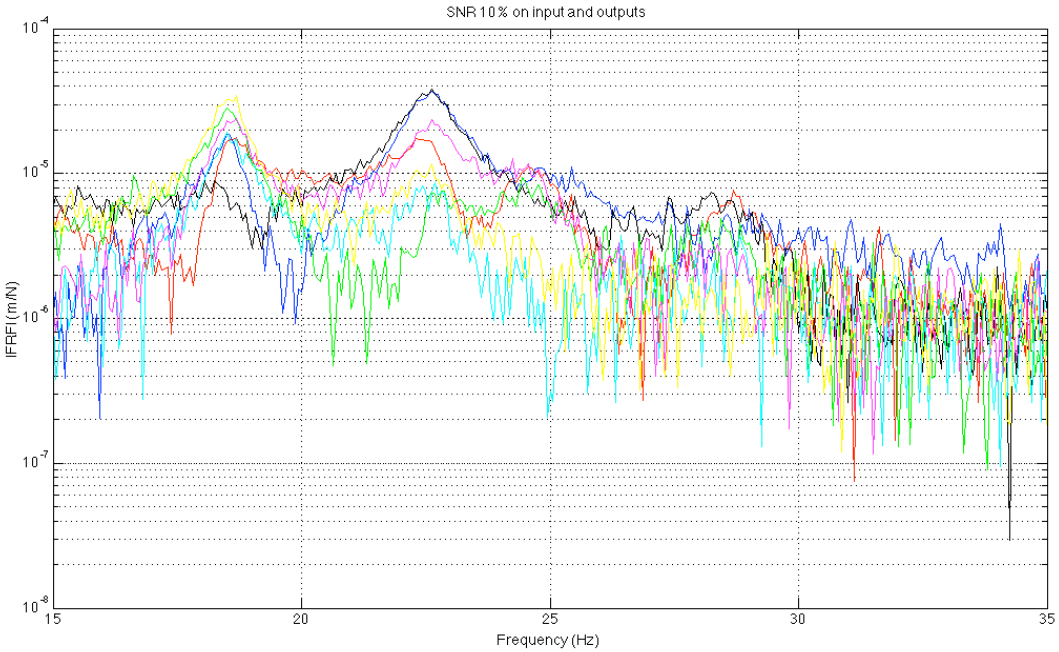

Fig. 3. Example of FRF (receptance) with noise on both input and outputs, e ¼ 1/10.

Table 3
Modal parameters and their standard deviations with 10% noise on both input and outputs (receptance)

Mode number k	1	2	3	4	5	6	7
f_k (Hz)	-	-	18.55	22.59	24.66	28.57	-
σ_f (Hz)	-	-	0.01	0.02	0.05	0.11	-
ζ_k (%)	-	-	8.17	5.77	5.22	4.55	-
σ_ζ (%)	-	-	0.26	0.18	0.38	0.75	-
MAC	-	-	0.998	0.997	0.984	0.951	-
σ_{MAC}	-	-	0.001	0.002	0.011	0.032	-

Frequency band: 15–35 Hz; maximum model order: 25.

Figure 4 and Table 4 show the results of an output only analysis. In principle, analysing cross spectra instead of FRFs is not different, apart from a scale factor given by the input force [12]. In practice it is reasonable to expect worse results on the basis of the simple observation that less information is elaborated. This is confirmed by Table 4 whose values are not as good as those of the input output analysis.

Of course the identification process achieves better results (not reported for brevity) when the added noise is not so large. Not surprisingly the damping ratios always show the largest discrepancies from the ideal values.

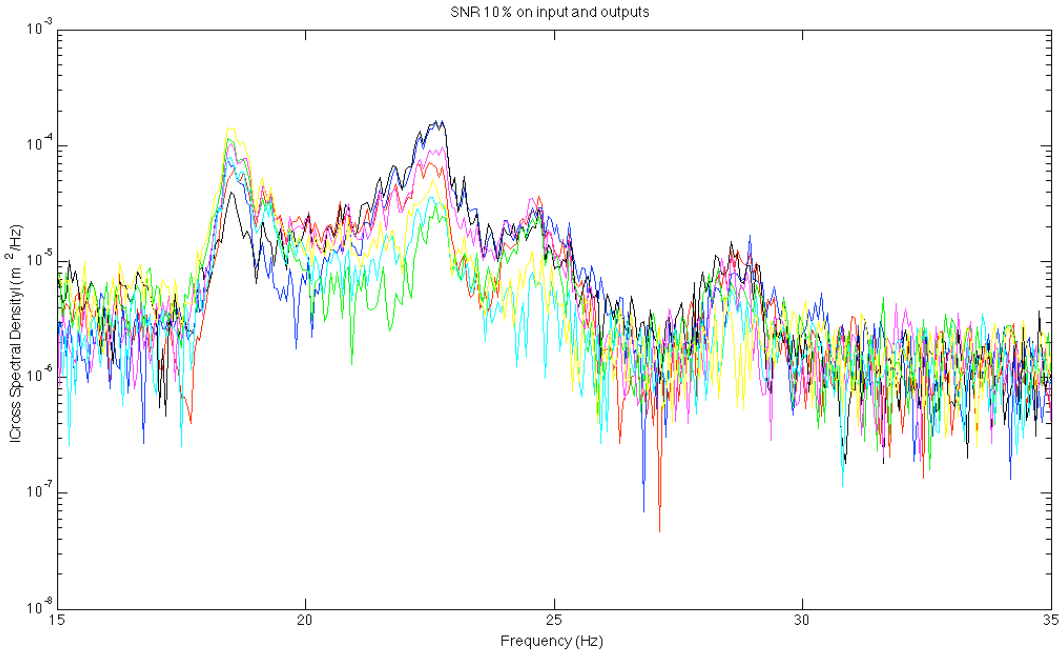

Fig. 4. Example of cross-spectrum (receptance) with 10% noise on outputs, e ¼ 1/10.

Table 4
Modal parameters and their standard deviations with 10% noise on outputs (output-only)

Mode number k	1	2	3	4	5	6	7
f_k (Hz)	-	-	18.57	22.55	24.75	28.61	-
σ_f (Hz)	-	-	0.04	0.06	0.11	0.17	-
ζ_k (%)	-	-	8.20	5.17	3.79	2.29	-
σ_ζ (%)	-	-	2.35	1.22	3.22	2.57	-
MAC	-	-	0.993	0.995	0.895	0.293	-
σ_{MAC}	-	-	0.004	0.003	0.088	0.253	-

Frequency band: 15–35 Hz; maximum model order: 25.

4. Experimental test

The proposed technique has also been tested on experimental data. The explanation of the laboratory apparatus is very short because all the information are still confidential; suffice is to say that the test rig consists of a metallic structure with an almost cylindrical shape in a free-free condition. The excitation (white noise) is imposed by a single electrodynamic shaker and the measured outputs are the triaxial accelerations of 40 points on eight cross sections of the cylinder, for a total of 960 time histories (and then NFRF=960). The essential information on the first four modes are reported in Table 5 where they are compared with the parameters extracted by the

canonical variate analysis. This technique is used as reference because its robustness and precision in elaborating real data has already been validated in many occasions – see for example [13].

The structure under test is nearly axisymmetric so that it is possible to excite modes with almost the same shape at almost the same frequency [14, 15]. In fact this is what happens for all the four modes herewith presented which show four companion modes (all within 1 Hz) with very similar, albeit rotated, mode shapes. Again the damping ratios estimated by the RFPZ method are larger than the expected.

Table 5
Modal parameters of the experimental rig

CVA		RFPZ		
Frequency (Hz)	Damping ratio (%)	Frequency (Hz)	Damping ratio (%)	$MAC_{CVA/RFPZ}$
19.03	0.60	18.98	2.21	0.96
23.71	0.37	23.69	1.54	0.99
57.71	0.58	57.65	1.16	0.82
73.58	0.39	73.62	0.50	0.97

5. Conclusion

This paper pretends to have plainly but exhaustively presented a modal parameter evaluation method written in the Z domain. Starting from SISO system, a total least squares procedure valid for MIMO (and output only) systems has been described together with some advices on how to achieve consistent modal parameters (frequency, damping ratios and modal constants) in a numerically efficient way. Among the stable poles appearing in a certain (limited) frequency band and computed by consecutively increasing the model order, a strategy to choose the most reliable mode is also suggested: the “best” pole is the one associated with the mode shape which, in the MAC sense, is most similar to all the others. The method has been validated through numerical and experimental examples which reveal very good performances but also some difficulties in the definition of the damping ratios.

Acknowledgements

The author gratefully thanks Dr. Stefano Marchesiello for the many helpful discussions and his elaboration of the experimental data with the CVA method.

References

[1] N.M.M. Maia, J.M.M. Silva, (Editors), Theoretical and Experimental Modal Analysis, Research Studies Press Ltd, Somerset, England, 1997.

[2] S.R. Ibrahim, E.C. Mikulcik, A time domain modal vibration test technique, The Shock and Vibration Bulletin, Vol. 43, No. 4 (1973), 21-37.

[3] E. Giorcelli, L. Garibaldi, B.A.D. Piombo, ARMAV techniques for traffic excited bridges, ASME Journal of Vibration and Acoustics (1998), 713-718.

[4] P. van Overshee, B. de Moor, Subspace identification for linear systems: theory, implementation, applications, Kluwer, Boston, 1996.

[5] J. Maeck, G. de Roeck, Description of the Z24 benchmark, Mechanical Systems and Signal Processing 17(2003), 127-131.

[6] M.H. Richardson, D.L. Formenti, Structural estimation from frequency response measurements using rational fraction polynomials, in: Proceedings of the First International Modal Analysis Conference IMAC, Orlando, Florida, U.S.A., 1982, pp 167-180.

[7] B. Peeters, H. Van der Auweraer, P. Guillaume, J. Leuridan,, The PolyMAX frequency domain method: a new standard for modal parameter estimation?, Shock and Vibration, 11(2004), 395-409

[8] S. Gade, N.B. Møller, H. Herlufsen, H Konstantin-Hansen, Frequency domain techniques for operational modal analysis, in: Proceedings of the International Modal Analysis Conference IMAC XXIV, St. Louis, Missouri, U.S.A., 2006, pp 1-10.

[9] P. Verboven, B. Cauberghe, P. Guillaume, Improved total least squares estimators for modal analysis, Computer and structures 83 (2005), 2077-2085.

[10] M.S. Allen, J.H. Ginsberg, A global, single-input–multi-output (SIMO) implementation of the algorithm of mode isolation and application to analytical and experimental data, Mechanical Systems and Signal Processing, 20(2006), 1090-1111

[11] J. Antoni, J. Schoukens, Practical guidelines for optimising the measurement of frequency response and coherence functions with digital spectral analysers, in: Proceedings of the International Conference on Noise and Vibration Engineering ISMA 2006, Leuven, Belgium, 2006, pp. 2451-2459.

[12] E. Parloo, Application of frequency-domain system identification techniques in the field of operational modal analysis, Ph.D thesis, Vrije Universiteit Brussel, Faculteit Toegepaste Wetenschappen, Brussel, Belgium, May 2003

[13] L. Garibaldi, S. Marchesiello, E. Bonisoli, Identification and up-dating over the z24 benchmark, Mechanical Systems and Signal Processing, 17(2006), 153-161

[14] J. Chung , J.M. Lee, Vibration analysis of a nearly axisymmetric shell structure using a new finite ring element, Journal of Sound and Vibration, Volume 219, Number 1 (1999), 35-50

[15] G. Chen, D. Fotsch, N. Imamovic, D. J. Ewins, Correlation methods for axisymmetric structures, in: Proceedings of IMAC XVIII: A Conference on Structural Dynamics, San Antonio, Texas, U.S.A.,

2000